REDUCED BASIS NUMERICAL HOMOGENIZATION FOR SCALAR ELLIPTIC EQUATIONS WITH RANDOM COEFFICIENTS: APPLICATION TO BLOOD MICRO-CIRCULATION

Yvon Maday, Noura Morcos, Toni Sayah

REDUCED BASIS NUMERICAL HOMOGENIZATION FOR SCALAR ELLIPTIC EQUATIONS WITH RANDOM COEFFICIENTS: APPLICATION TO BLOOD MICRO-CIRCULATION

YVON MADAY*, NOURA MORCOS†, AND TONI SAYAH‡

Abstract. We consider a non periodic homogenization model designed to simulate the blood flow at the level of the micro-vascularised tissues. We solve elliptic partial differential equations with two length-scales on the domain and we use the reduced-basis method to speed up the numerical resolution. Finally, we show numerical results and comparisons in 2D and 3D.

Key words. Porous media, stochastic homogenization, reduced basis method, microcirculation, blood flow

AMS subject classifications. 74Q05, 74SQ5, 65N15, 35J20

1. Introduction. Our goal in writing this paper is to develop a novel numerical technique for approximating the solution of second order scalar elliptic boundary value problems with highly oscillating coefficients amenable to take into account some randomness. Such mathematical models are involved in many applications, including thermal diffusion in porous media, constitutive laws of composite materials, behavior of biological tissues. The high oscillations are represented by a small parameter denoted by $\varepsilon \in \mathbb{R}^+$ that actually may represent several distinct scales, ε being only a notation for representing the small components that are present in the phenomenon. In what follows we only focus on the two scale problem (one macro scale and one micro scale). Solving directly such problems is generally quite expensive, even impossible. For instance, with plain finite element methods, since the discretization mesh should be small enough in order to represent well the oscillations meaning that the mesh size should be smaller than ε, the computation load would scale at least as $\mathcal{O}(\varepsilon)^{-3}$ in 3-dimensions, which is difficult to manage especially when $\varepsilon \to 0$.

It should first be noticed that, for most of the practical applications, there is only one problem to be solved, corresponding to a unique value of ε say $\varepsilon = \varepsilon_0$, however, if ε_0 is very tiny, with respect to the macroscopic size of the problem, it may be smart to invent a family of problems depending on ε and discover the asymptotic limit behavior of the solution as $\varepsilon \to 0$, we then speak about homogenization theory and homogenized problem.

In such cases, the determination and the mathematical justification of the limit behavior is more or less known in some particular cases related to the dependency of the problem in ε, with a full rigorous theory that is available only in few cases. Recent advances have allowed to incorporate randomness in the structure of the oscillations improving the range of applications of these models. In order to go even further, numerical homogenization techniques have been introduced to cope with some current holes in the theory. This subject is very much actual and active due to the variety of applications that can be considered.

*1-UPMC Univ Paris 06, UMR 7598, Laboratoire Jacques-Louis Lions, F-75005, Paris, France.
2-Division of Applied Mathematics, Brown University, Providence, RI, USA.
(maday@ann.jussieu.fr)

†Faculté des Sciences, Université Saint-Joseph, B.P 11-514 Riad El Solh, Beyrouth 1107 2050, Liban. (morcos@ann.jussieu.fr).

‡Faculté des Sciences, Université Saint-Joseph, B.P 11-514 Riad El Solh, Beyrouth 1107 2050, Liban. (tsayah@fs.usj.edu.lb).

In a nutshell, most of the homogenization techniques, when two scales are separated, allow to replace the resolution of one problem with two scales into the resolution of two classes of coupled problems each dealing with one scale, in particular the fine scale problem depends on the large scale and its solution enters in the definition of the large scale limit problem. Numerical homogenization techniques then require the simulation of a huge number of micro scale problems. This paper builds up on the contribution by Boyaval [12] that proposes and illustrates the use of reduced basis methods for solving these micro scale problems. Reduced basis methods introduced in [17, 28], offer a particularly well suited solution to the challenges of this many-query framework, aiming to achieve efficiently the simulation of this huge amount of similar problems. A fundamental observation and assumption utilized by RBM is that the solutions at the micro scale level constitute a family of low dimension parameterized by the macro scale variable. Therefore, one can expect that every particular solution, at the micro scale level, can be well approximated by a finite and low dimensional vector space. In the context of the RBM, this low dimensional space is chosen as being spanned by (very well) approximated solutions to the same problem for very few, well chosen, macro scale spacial variables. In addition, we incorporate in this paper one important new feature: the stochastic dimension in the definition of the microscopic structure.

In the second part of this paper, we present the particular problem that actually has led us to develop the stochastic two scale homogenization: it is related to the modeling of blood flow at the level of the micro-vascularised tissues. Many example referring to homogenization exist in the literature describing such models of microcirculation that account for the highly oscillating media composed of microstructures. Biological tissues are certainly a place where randomness is illustrated and mathematical models have to account for this feature. The model we propose here enters in this stochastic homogenization frame and leads to methods for constructing the limit homogenized behavior. The stochastic frame and the particularity of the material involving components in which the flow does not exist, lead to some new specific difficulties and contributions (in terms of numerical analysis and limit behavior) that we handle here.

2. Basics of homogenization theory.

2.1. Abstract homogenization. Let $\mathcal{D}$ be an open piecewise $\mathscr{C}^1$ bounded domain of $\mathbb{R}^d$ with a boundary $\Gamma = \partial\mathcal{D}$. We denote by $\vec{n}$ the exterior unit normal to Γ defined a.e. and we assume that Γ is decomposed into two non overlapping open parts Γ_D and Γ_N. We are interested in the behavior of a sequence of scalar functions u^ϵ that satisfy the following scalar elliptic equation in divergence form with random coefficients

$$\begin{aligned} &-\mathrm{div}(A^\epsilon(.;\omega)\ \nabla u^\epsilon(.;\omega)) = f, \quad \text{in } \mathcal{D}, \\ &u^\epsilon|_{\Gamma_D} = g_D; \quad A^\epsilon \nabla u^\epsilon . \overrightarrow{n}|_{\Gamma_N} = g_N; \end{aligned} \tag{2.1}$$

for a sequence of scalars $\epsilon > 0$. Here $\omega \in \Omega$, with $(\Omega, \mathcal{F}, \mathbb{P})$ being a probability space over Ω. We assume that, e.g., $f \in L^2(\mathcal{D})$, $g_D \in H^{1/2}(\Gamma_D)$ and $g_N \in L^2(\Gamma_N)$ and we look for the asymptotic limit of the sequence $u^\epsilon(.;\omega)$ when $\epsilon \to 0$. For every $\epsilon > 0$ and almost surely in ω, we assume that $A^\epsilon(.;\omega) \in L^\infty(\mathcal{D}, \mathcal{M}_{\alpha,\beta})$, where $\mathcal{M}_{\alpha,\beta}$ is the set of uniformly positive definite square matrices with uniformly positive definite inverse,

that is, matrices B satisfying, for all $x \in \mathcal{D}$,

$$\begin{array}{l} 0 < \alpha|\xi|^2 \leq < B(x)\xi, \xi >, \forall \xi \in \mathbb{R}^d, \\ 0 < \beta|\xi|^2 \leq < (B(x))^{-1}\xi, \xi >, \forall \xi \in \mathbb{R}^d. \end{array} \tag{2.2}$$

The problem (2.1) is almost surely well posed and for every $\epsilon > 0$, there exists a unique solution $u^\epsilon(.;\omega) \in H^1(\mathcal{D})$ verifying the relation

$$||u^\epsilon(.,\omega)||_{H^1(\mathcal{D})} \leq C(\mathcal{D},\alpha,\beta)\left[||f||_{L^2(\mathcal{D})} + \|g_D\|_{H^{1/2}(\Gamma_D)} + \|g_N\|_{L^2(\Gamma_N)}\right].$$

Classical results about H-convergence (see e.g. [22], [25], [2], [7]) state that, under the above hypothesis, there exists a subsequence, still denoted as ε, and a homogenized matrix $A^*(.,\omega) \in L^\infty(\mathcal{D}, \mathcal{M}_{\alpha,\beta})$ such that, almost surely in ω, $A^\varepsilon(.,\omega)$ H-converges towards $A^*(.,\omega)$. Let us restrict ourselves momentarily to the case where $\Gamma_N = \emptyset$ and $g_D = 0$, since homogenization does not depend on the type of boundary conditions that are imposed (nor on f). In this case, this means that, for $\varepsilon \to 0$, the limit being true in $\mathscr{D}'(\mathcal{D};\mathbb{R}^n)$

$$\begin{array}{r} u^\varepsilon(.,\omega) \rightharpoonup u^*(.,\omega), \\ A^\varepsilon \nabla u^\varepsilon(.,\omega) \rightharpoonup A^* \nabla u^*(.,\omega), \end{array} \tag{2.3}$$

where $u^*(.,\omega)$ is the solution to

$$\begin{array}{l} -\mathrm{div}(A^*(.;\omega)\ \nabla u^*(.;\omega)) = f, \quad \text{in } \mathcal{D}, \\ u^* = 0 \quad \text{on } \partial\mathcal{D}. \end{array} \tag{2.4}$$

It should be noticed that, in many cases, the matrix A^* (and thus u^*) is actually deterministic: this remarkable property of the matrix A^* results from natural assumptions of stationarity and ergodicity. However, it is possible to build materials for which such a stochastic averaging effect does not hold.

Besides, except in some particular cases (e.g. periodic case, or in the stochastic frame of [29]) an explicit formula for the limit A^* is not available which leaves a large room for investigation. Actually the result above goes only a little bit further by introducing the following abstract elements defined implicitly as the solutions $\hat{w}_i^\varepsilon$ to the problems

$$\begin{cases} -\mathrm{div}(A^\epsilon(.;\omega)\ \nabla \hat{w}_i^\varepsilon(.;\omega)) = -\mathrm{div}(A^*(.;\omega)\ \vec{e}_i) \quad \text{in } \mathcal{D}, \\ \hat{w}_i^\varepsilon(.;\omega) = x_i \quad \text{on } \partial\mathcal{D}, \end{cases} \tag{2.5}$$

where $(\vec{e}_i)_{1\leq i\leq d}$ denotes the canonical basis of $\mathbb{R}^d$, and $(x_i)_{1\leq i\leq d}$ the associated coordinates.

We then have the limit properties almost surely in ω

$$\hat{w}_i^\varepsilon(.;\omega) \rightharpoonup x_i \tag{2.6}$$

and

$$A^\epsilon(.;\omega)\ \nabla \hat{w}_i^\varepsilon(.;\omega) \rightharpoonup A^* \vec{e}_i. \tag{2.7}$$

In addition (see e.g. [2]), these solutions, $\hat{w}_i^\varepsilon$, named "oscillating test functions" allow to get the following corrector result:

$$\nabla u^\varepsilon(.;\omega) = \sum_{i-1}^{d} \nabla \hat{w}_i^\varepsilon(.;\omega) \frac{\partial u^*(.;\omega)}{\partial x_i} + r^\varepsilon(.,\omega), \tag{2.8}$$

where $r^\varepsilon(.,\omega)$ converges strongly to zero in $L^1(\mathcal{D})$. It results that, whenever $u^*(.;\omega) \in H^2(\mathcal{D})$

$$u^\epsilon(.;\omega) = u^\star(.;\omega) + \sum_{i=1}^{d} (\hat{w}_i^\varepsilon(.;\omega) - x_i) \frac{\partial u^*(.;\omega)}{\partial x_i} + R^\epsilon(.,\omega), \tag{2.9}$$

where the remainder $R^\varepsilon(.,\omega)$ converges strongly to zero in $W^{1,1}(\mathcal{D})$. This powerful theory is somehow weakened for the applications by the fact that A^* is hard to construct.

The above analysis has lead Kozlov [23] to suggest a change of variable, the so called "harmonic coordinates". This has been further used by [21], [2], [16], [18] in various forms in order to propose a numerical integration method for approximating the construction of A^* (giving rise to the methods that are known now as MsFEM, HMM..) .

In the following section, we restrict the generality of the frame and assume that there exists a clear separation between the only 2 scales in presence and that the situation is either periodic or a (stochastic) perturbation of a periodic situation.

2.2. Two-scale homogenization. Let us now introduce the two-scale homogenization theory (without randomness as for now) to get explicit expressions for the homogenized problem ([1], [26]). We assume that the tensors A^ϵ are functions of two coupled variables on the set locally defined by a fast microscopic variable $\epsilon^{-1}x$ coupled with the slow macroscopic variable x in $\mathcal{D}$.

$$A^\epsilon(x) = A(x, \frac{x}{\epsilon}), \tag{2.10}$$

where $A(x,.)$ is $Y = [0,1]^d$-periodic, $x \in \mathcal{D}$ and $A \in L^\infty(\mathcal{D}, \mathcal{M}_{\alpha,\beta})$. We denote by x the macroscopic variable and by $y = \dfrac{x}{\epsilon}$ the microscopic variable. As $A(x, \dfrac{x}{\epsilon})$ is locally periodic, one possible manner to get explicit expression for the homogenized problem is to perform a formal two-scale analysis with the following Ansatz:

$$u^\epsilon(x) = \sum_{j=0}^{+\infty} \epsilon^j u_j(x, \frac{x}{\epsilon}) = u_0(x, \frac{x}{\epsilon}) + \epsilon u_1(x, \frac{x}{\epsilon}) + \epsilon^2 u_2(x, \frac{x}{\epsilon}) + ... \tag{2.11}$$

where, for any $x \in \mathcal{D}$, the functions $u_j(x,.)$ are Y-periodic. Inserting the Ansatz (2.11) into equation (2.1) allows us to write u^ϵ as:

$$u^\epsilon = u^\star + \epsilon \sum_{i=1}^{d} w_i \partial_i u^\star + r_\epsilon, \tag{2.12}$$

where $(w_i(x,.))_{1 \le i \le d}$ are d Y-periodic, with zero average over Y, cell functions, parameterized by their macroscopic position $x \in \mathcal{D}$ that verify the following n cell problems (that now can be used as it is explicit)

$$-\operatorname{div}_y(A(x,y)[\vec{e}_i + \nabla_y w_i(x,y)]) = 0, \forall y \in Y. \tag{2.13}$$

The function $u_0 = u^\star$ does not depend on the fast variable $y = \epsilon^{-1}x$ any more and verifies the homogenized problem:

$$\begin{cases} -\mathrm{div}(A^*(x)\ \nabla u^*(x)) = f,\ \forall x \in \mathcal{D}, \\ u^*|_{\Gamma_D} = g_D, \\ A^*(x)\ \nabla u^*.\overrightarrow{n}|_{\Gamma_N} = g_N. \end{cases} \tag{2.14}$$

the entries $(A^*_{ij}(x))_{1\leq i,j\leq d}$ of the homogenized matrix A^* can now be explicitly computed with the cell functions $w_i(x,.)$,

$$A^*_{ij}(x) = \int_Y A(x,y)(\vec{e}_i + \nabla_y w_i(x,y))\vec{e}_j dy, \tag{2.15}$$

where, provided $u^\star \in W^{2,\infty}(\mathcal{D})$, the correction error r_ϵ can be estimated to locally scale as ϵ (far enough from the boundary), and to globally scale as $\sqrt{\epsilon}$ (see [1]):

$$\begin{aligned} &||r_\epsilon||_{H^1_{\Gamma_D}(\omega)} \leq C_1\epsilon||u^*||_{W^{2,\infty}(\omega)}, \forall w \overset{c}{\subset} \mathcal{D}, \\ &||r_\epsilon||_{H^1_{\Gamma_D}(\mathcal{D})} \leq C_2\sqrt{\epsilon}||u^*||_{W^{2,\infty}(\mathcal{D})}, \end{aligned} \tag{2.16}$$

with constants C_1 and C_2 depending only on $\mathcal{D}$.
The local periodicity assumption (2.10) allows to completely determine the homogenized problem through explicit two-scale expressions. The derivation of the homogenized equation in the case of locally periodic coefficients serves as a basis in many numerical homogenization strategies. For the algorithm concerning the two-scale homogenization strategy, we refer to [16].

For the numerical approximation of these problems, finite element methods can be proposed. The construction of the associated stiffness matrix of the macroscopic problem requires the construction of A^* at every point in $\mathcal{D}$ or more precisely at every integration points on (say) each tetrahedra composing the macroscopic mesh; in what follows we shall denote this set as $\mathscr{M}(\mathcal{D})$. Each of these evaluations involves the resolution of a micro scale problem (2.13). If a standard approximation method is used at the level of the microscopic problem, this may be a very expensive strategy, even though all of these problems are mutually independent and thus can be solved in a parallel way. This has motivated the use of reduced basis method to solve this series of macroscopic problems (see [12]).

3. The reduced-basis method for non periodic homogenization problems.

3.1. Basics for the reduced-basis methods for 2-scale homogenization. Let us first write the problem of interest in an abstract form so as to explain the basics of the Reduced Basis Method (RBM) more easily.

Let $\mathcal{X}$, be the quotient space $H^1(Y)/\mathbb{R}$ homeomorphic to the space of all Y-periodic functions with zero average over Y, that belong to the Sobolev space $H^1(Y)$. $\mathcal{X}$ is equipped with the norm $||u||_{\mathcal{X}} = (\int_Y \nabla u.\nabla u)^{\frac{1}{2}}$.

For any integer i, $1 \leq i \leq d$, the i-th cell problem (2.13) for the cell functions $w_i(x,.)$ rewrites in the following weak form:

$$\begin{cases} \text{Find } w_i(x,.) \in \mathcal{X} \text{ solution for:} \\ a(w_i(x,.), v; x) = f_i(v; x), \quad \forall v \in \mathcal{X}. \end{cases} \tag{3.1}$$

where $x \in \mathcal{D}$ appears to play the role of a parameter, a is a continuous and coercive bilinear form in $\mathcal{X} \times \mathcal{X}$ parameterized by $x \in \mathcal{D}$ defined as

$$a(u, v; x) = \int_Y A(x, y) \nabla u(y).\nabla v(y) dy,$$

and f_i are linear and continuous forms defined as

$$f_i(v; x) = -\int_Y A(x, y)\vec{e}_i.\nabla v(y) dy, \quad 1 \leq i \leq d.$$

For many problems depending on some parameter (e.g. for an optimization problem, a control problem, an inverse problem or, like here for the resolution of the small scale problem) the set of all solutions forms a manifold of very small Kolmogorov dimension. In such cases, a reduced basis method can be implemented provided some further ingredients (albeit less fundamental see [14]) are available. Among these ingredients the existence of a cheap error estimator is helpful. Then the RBM can be implemented into two steps through what is known as *offline/ online approach*. Let us explain it in our frame: Let us first introduce, for any i, the set of all solutions to problem (2.13) $\mathscr{S}_i = \{w_i(x, .), x \in \mathcal{D}\}$ that is a manifold over $\mathcal{D}$.

The first step — that may be expensive but done once and for all and, may be, before the RBM approximation is actually used — consists in choosing, e.g. through a greedy method, conducted with an available error estimator, the values of x_n that are to be chosen to enrich at most the approximation quality of $\mathcal{X}_{iN}$ for $\mathscr{S}_i$ (see [30] and algorithm 3.2 below). For these values, we then approximate the associated solutions $w_i(x_n, .)$, $n = 1, \ldots, N$ with some classical (e.g. finite element method) accurate enough. After this is done, still in the *offline* stage, some scalar products are computed and bilinear forms working on $w_i(x_n, .)$, $n = 1, \ldots, N$, so that the evaluation of the RBM stiffness matrix will be rapidly achieved. Most of the times, this will involve the use of the Empirical Interpolation Method (EIM) (see [4], [19]).

In a second step, called *online* stage, for every new values of the integration point $x \in \mathcal{D}$, and any i, $1 \leq i \leq d$, the Galerkin approximation $w_{iN}(x, .) \in \mathcal{X}_{i,N} = \text{Span}\{w_i(x_n, .), n = 1, \ldots, N\}$ of $w_i(x, .)$ satisfies:

$$a(w_{iN}(x, .), v; x) = f_i(v; x), \quad \forall v \in \mathcal{X}_{i,N}. \tag{3.2}$$

The stiffness matrix $(a(w_{iN}(x_n, .), w_{iN}(x_m, .); x))_{n,m}$ is then built *online* in a very few operations (since every thing is prepared for this in the *offline* stage) and the problem is solved in $\mathcal{O}(N^3)$ operations, providing a RBM approximation for $w_i(x, .)$, possibly with an associated error estimate. We refer to [30] for a general presentation.

The RBM approach for the parameterized cell problems (2.13) should significantly decrease the expense of computations in terms of CPU time for the homogenization problems even if we take into account the construction time of the offline stage as we shall see latter.

3.2. Approximation of the limit coefficients and *a posteriori* **error analysis.** The macroscopic stiffness matrix is thus computed by using, at every point x involved in the macro scale numerical integration $\mathscr{M}(\mathcal{D})$, the micro scale functions $w_{iN}(x, y)$. This is done by the following quantities:

$$A^*_{ij,N}(x) = \int_Y A(x, y)(\vec{e}_i + \nabla_y w_{iN}(x, y)).\vec{e}_j dy = s_{ij,N}(x) + \int_Y A(x, y)\vec{e}_i.\vec{e}_j dy, \tag{3.3}$$

where $(s_{ij,N})_{1\leq i,j\leq d}$ is defined by:

$$s_{ij,N}(x) = -f_j(w_{i,N}(x,.);x) = \int_Y A(x,y)\vec{e}_j, \nabla w_{i,N}(x,y)dy. \tag{3.4}$$

Let us recall now the two following theorems which enable us to define the a *posteriori* bounds error of this matrix.

THEOREM 3.1. *[12] For $1 \leq i \leq d$, we define the a posteriori error estimation $\Delta_N(w_i(x,.))$ by:*

$$\Delta_N(w_i(x,.)) = (\parallel a(w_i(x,.) - w_{iN}(x,.),.;x) \parallel_{\mathcal{X}'})/\alpha,$$

and the corresponding effectivities $\eta_i(x)$ by

$$\eta_i(x) = \Delta_N(w_i(x,.))/ \parallel w_i(x,.) - w_{i\mathrm{N}}(x,.) \parallel_{\mathcal{X}} .$$

They satisfy the N-independent inequalities:

$$1 \leq \eta_i(x) \leq \frac{\beta^{-1}}{\alpha}.$$

THEOREM 3.2. *[12] Let $w_i(x,.)$ (resp. $w_j(x,.)$) be a solution of the problem $(3.1)_i$ (resp. $(3.1)_j$) and $w_{i\mathrm{N}}(x,.)$ (resp. $w_{j\mathrm{N}}(x,.)$) a solution of the problem $(3.2)_i$ (resp. $(3.2)_j$) with $i \neq j$, we have*

$$\mid s_{ij,N}(x) - s_{ij}(x) \mid \leq \Delta^s_{ij,N}(x),$$

with

$$\Delta^s_{ij,N}(x) = \frac{\parallel a(w_i(x,.) - w_{i\mathrm{N}}(x,.),.;x) \parallel_{\mathcal{X}'} \parallel a(w_j(x,.) - w_{j\mathrm{N}}(x,.),.;x) \parallel_{\mathcal{X}'}}{\alpha}.$$

Remark. *The above definitions (e.g. $\Delta_N(w_i(x,.))$) involve a norm in $\mathcal{X}'$ of the residuals ($a(w_i(x,.) - w_{iN}(x,.),.;x) = f_i(.;x) - a(w_{iN}(x,.),.;x)$) that may be expensive, a priori, to evaluate but for which there also exists an offline/ online strategy that we shall not dwell upon and refer to [30]. Such a strategy allows to perform these evaluations in $\mathcal{O}(N^2)$ operations.*

To conclude on this matter, let us summarize the construction of the reduced basis

Algorithm 1:

1. *For some given x_1, we compute the finite element approximation $w_{i,h}(x_1,.)$ of $w_i(x_1,.)$ using* (3.1).
2. *We set* $\ell = 1$, and $\xi_1 = \dfrac{w_{i,h}(x_1,.)}{\parallel w_{i,h}(x_1,.) \parallel_{\mathcal{X}}}$, *the first reduced function.*
3. Then while $\ell < N$:

(a) *we compute for every* $x \in \mathscr{M}(\mathcal{D})$ the *reduced basis approximations* $w_{i,\ell}(x,.)$ in $\mathcal{X}_{i,\ell} = \text{span}\{\xi_j, 1 \leq j \leq \ell\}$ for the cell problem (3.2).

(b) *for* $x_{\ell+1} = \underset{x\in\mathscr{M}(\mathcal{D})}{\text{argmax}} \dfrac{\Delta^s_{ii,\ell}(x)}{\| w_{i,\ell}(x,.) \|_{\mathcal{X}}}$ *we compute the finite element approximation* $w_{i,h}(x_{\ell+1},.)$ of $w_i(x_{\ell+1},.)$ using the (micro) finite element approximation of (3.1).

(c) *we set* $\xi_{\ell+1}(y) = \dfrac{R_{\ell+1}(y)}{\| R_{\ell+1}(y) \|_{\mathcal{X}}}$, the $(\ell+1)^{th}$ *reduced basis, where* $R_{\ell+1}$ *is the remainder of the projection of* $w_{i,h}(x_{\ell+1},.)$ *on the* ℓ*-dimensional reduced basis*:

$$R_{\ell+1}(.) = w_{i,h}(x_{\ell+1},.) - \sum_{k=1}^{\ell} (w_{i,h}(x_{\ell+1},.), \xi_k)_{\mathcal{X}}\ \xi_k(.).$$

(d) *we do* $\ell = \ell + 1$ *and go back to* (*a*).

3.3. Numerical results. In this subsection, we present some numerical results illustrating different points presented previously. We consider a case where $d = 3$, the domain $\mathcal{D} =]0;1[^3$ and the permeability is isotropic and diagonal with coefficients on the diagonal equal to

$$a_{ii}(x,y) = 4 + \cos(2y_1)x_1 + \cos(2y_2)x_2 + \cos(2y_3)x_3.$$

We first check that the complexity of the manifold of all micro scale solutions when x varies is small. For this analysis, we perform a large number of finite element approximations of the cell problem for various values of x. The computations are performed with the software FreeFem++ [20], using $\mathbb{P}_1$ finite elements. The considered mesh contains 48.000 elements (tetrahedra). The following figures show the decreasing of the relative maximal error

$$\mathcal{A}_N = \max_{1\leq i\leq 3, x\in\mathscr{M}(\mathcal{D})} \frac{\Delta_N(w_i(x,.))}{\| w_i(x,.) \|_{\mathcal{X}}},$$

the relative error of the cell functions

$$\mathcal{B}_N = \max_{1\leq i\leq 3, x\in\mathscr{M}(\mathcal{D})} \frac{\| w_i(x,.) - w_{iN}(x,.) \|_{\mathcal{X}}}{\| w_i(x,.) \|_{\mathcal{X}}}$$

and the relative error of s_{ij},

$$\mathcal{C}_N = \max_{1\leq i,j\leq 3, x\in\mathscr{M}(\mathcal{D})} \frac{|s_{ij}(x) - s_{ij,N}(x)|}{|s_{ij}(x)|},$$

with respect to the number of basis functions.

As we can see in those figures (Figures 3.1 and 3.2), the considered relative errors decrease rapidly with respect to the number of basis and the one corresponding to $s_{ij,N}$ converge twice as fast as the others.

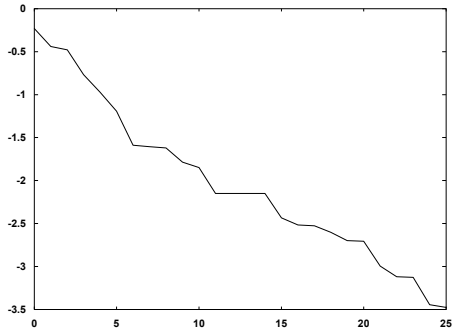

FIG. 3.1. *$\mathcal{A}_N$ in logarithmic scale with respect of N*

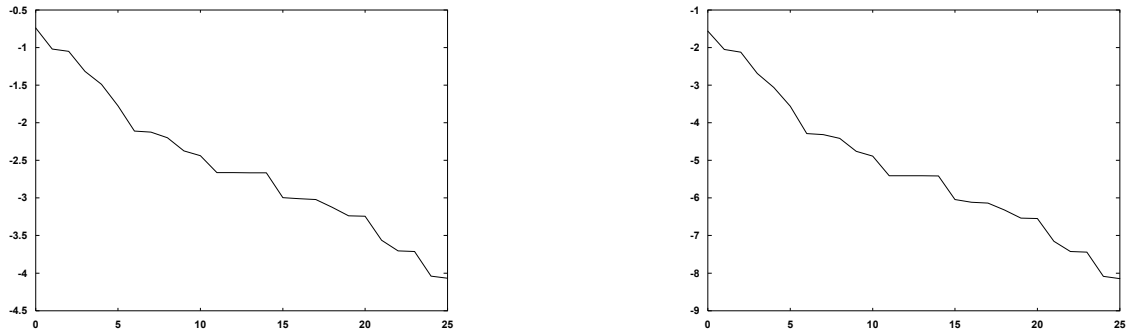

FIG. 3.2. *$\mathcal{B}_n$ and $\mathcal{C}_N$ in logarithmic scale with respect of N*

NB	$\mathcal{N}_\mathcal{Y}$	$\mathcal{N}$	RBM	FEM
10	125	216	1.5 s	140 s
10	1,000	216	1.5 s	1,100 s
10	125	9,261	95 s	8,800 s
10	1,000	9,261	95 s	70,000 s

FIG. 3.3. *Comparison between the classical finite elements and the reduced basis method in three dimensional.*

The table (Fig. 3.3) shows the CPU time (in seconds) given by the Freefem++ code to approximate the FE matrix for the homogenized problem either with a direct FE approach or with a RB method for a porous medium, where NB is the bases number, $\mathcal{N}_\mathcal{Y}$ is the number of the degrees of freedom of the cell, $\mathcal{N}$ is the number of the degrees of freedom of $\mathcal{D}$, *offline part* is the time of the bases construction, RBM is the time of the calculation of A^* using the reduced basis method and FEM is the time of the calculation of A^* using the finite element method.

We can notice that the RB method is much faster than the FEM which shows the efficiency of the RB method, even if we include the offline part, that corresponds to solving less than N^2 finite element solutions which is far less than twice the RBM work, even in the largest case in table 3.3 ($\mathcal{N}_\mathcal{Y} = 1,000$, $\mathcal{N} = 9,261$).

3.4. About randomness. In order to account for some randomness we choose an approach inspired by [8] where the randomness is incorporated in the description of the microstructure by using random deformations of the periodic coefficients

previously defined. We thus introduce a (random) parameter dependent function $\phi_\theta(y) = -2\theta y^3 + 3\theta y^2 + (1-\theta)y$ which is a simple one to one mapping from $[0,1]$ onto $[0,1]$ for every $\theta \in]-2,1[$.

Starting from a matrix $\hat{A}(y)$, the definition of the previous coefficients $A(x,y)$ in every cell is obtained, for every $1 \leq i \leq d$, by replacing each component y_i by $\phi_\theta(y_i)$ (we denote by $\Phi_\theta(y) = (\phi_\theta(y_1), \ldots, \phi_\theta(y_n)))$.
The coefficients are then

$$A(x,y;\theta) = \hat{A}(\Phi_{\theta(x,\omega)}(y)) \tag{3.5}$$

meaning that at any macroscopic point x, the associated cell-matrix is randomly modified through the mapping $\Phi_{\theta(x,\omega)}$.

For the simulation, this does not modify much the homogenization approach : At every point $x \in \mathscr{M}(\mathcal{D})$ we compute the micro scale problem (2.13) with a RBM based on a discrete space $\mathcal{X}_N$ that is constructed, as explained before, but where the parameter x appears now through θ.

Note that this is a *model* for taking into account some randomness, it is somehow similar to [8] but differs from it in the sense that here we do not construct a global random map over $\mathbb{R}^d$ to modify the periodic cell structures. Since we are mainly interested in numerical simulations, this cell by cell modification is sufficient. It is out of the scope of this first paper to make the actual link between these two versions or the theory developed in [10, 9] and further understand to what extent the discrete version presented here is an approximation of the continuous random stationary diffeomorphism introduced in [8]. Note that, in opposition to these cited papers, our limit approximation remains random while the limit problem and solution of [8] are deterministic (note however that this is also the case of the approximation proposed in [15] that remains also random). We plan to analyze the link between these two notions in a future paper.

The random macroscopic stiffness matrix is now computed by using, at every point x involved in the macro scale numerical integration $\mathscr{M}(\mathcal{D})$, the micro scale functions $w_{iN}(x, \Phi_{\theta(x,\omega)}(y))$. This is done by the following quantities:

$$\begin{aligned} A^*_{ij,N}(x,\theta) &= \int_Y \hat{A}(\Phi_{\theta(x,\omega)}(y))(\vec{e}_i + \nabla_y w_{iN}(x, \Phi_{\theta(x,\omega)}(y))).\vec{e}_j dy \\ &= s_{ij,N}(x,\theta) + \int_Y \hat{A}(\Phi_{\theta(x,\omega)}(y))\vec{e}_i.\vec{e}_j dy. \end{aligned} \tag{3.6}$$

Remark. *Note that, as is often the case when changes of variables are involved as a parameter for RB approximation the manifold of solutions is defined as*

$$\widehat{\mathscr{S}_i} = \{\widehat{w}_i(x,.;\theta) = w_i(x, [\Phi_{\theta(x,\omega)}]^{-1}(.)), x \in \mathcal{D}\} \tag{3.7}$$

rather than the original

$$\mathscr{S}_i = \{w_i(x,.), x \in \mathcal{D}\};$$

since, most often, the Kolmogorov dimension is smaller in the former case.

Remark. *Note that the matrix $\hat{A}$ could also depend on x, the random cell matrix would then be*

$$A(x,y;\theta) = \hat{A}(x, \Phi_{\theta(x,\omega)}(y));$$

there would then be two parameters for the RB frame: x and θ.

4. Application. The blood microcirculation in the capillaries can be modelled by a flow in a porous media which is governed by the Darcy law, established by Henri Darcy (1857) as a result of extensive work on the water flow in a layer of sand filter. Considering that the blood is a Newtonian incompressible fluid, we can build the corresponding problem modelling the blood flow in the capillaries in 2D and 3D, using the Darcy law in a domain decomposed in small cells having the same small size ϵ but different structures in each cell:

$$\left\{ \begin{array}{rcl} v^\epsilon & = & -A^\epsilon \nabla p^\epsilon, \\ \mathrm{div} v^\epsilon & = & 0. \end{array} \right. \tag{4.1}$$

Where v^ϵ is the velocity, p^ϵ the pressure and A^ϵ a symmetric tensor representing the quotient between the permeability and the viscosity of the blood. We suppose that the viscosity has a constant value on the domain. There are many applications of the Darcy law in the biology, for instance Vankan and Van Donkelaar [31] describe the blood circulation in the muscles by five layers (arteries, arterioles, capillaries, venules and veins) using Darcy law to represent horizontal flux in each layer, and Baeur D. & all [5, 6] have described a vascular network by a three-layer model in order to model the effect of the irritation on the microcirculation.

For a flow in a periodic porous medium, A^ϵ can be represented by a periodic function $A^\epsilon(x) = A(\frac{x}{\epsilon})$ ([3, 7]). To model a porous media with a slight modification of structures from one cell to the other, the tensor A^ϵ can be considered as a function of two variables $A(x, \frac{x}{\epsilon})$ (see section 2.2).

4.1. Description of the model. In this section we aim at simulating the blood flow in a network of capillaries. The model we propose will be represented by a non uniform two scale system with cells of size ε where the part of the cell representing the capillaries is permeable and connects the adjacent cells, while the remaining part is not, and thus is represented by a permeability tensor which almost vanishes on these regions of the domain. Each cell will be defined as the (random) deformation of a reference cell: let $\hat{y} = (\hat{y}_1, \ldots, \hat{y}_d)$ and let $\hat{\Lambda} = [0,1]^d$ be the reference cell where the permeability is defined as follows: $\forall \hat{y} \in [0,1]^d$,

$$\widehat{K}(\hat{y}) = \left(\widehat{K}_{ij}(\hat{y}) \right)_{0 \leq i,j \ \leq d},$$

with $\widehat{K}_{ij} = 0$ if $i \neq j$ and

$$\widehat{K}_{ii}(\hat{y}) = \frac{1}{\sigma\sqrt{2\pi}} e^{-\frac{1}{2}(\frac{\hat{y_1} - 0.5}{\sigma})^2} + \cdots + \frac{1}{\sigma\sqrt{2\pi}} e^{-\frac{1}{2}(\frac{\hat{y_d} - 0.5}{\sigma})^2} + \varsigma,$$

where $\sigma = 0.07$ and $0 < \varsigma << 1$. We denote by $\hat{\mathcal{X}} = H^1_\sharp(\hat{\Lambda})/\mathbb{R}$.

In order to build a random porous media, we will vary randomly the permeability as explained in subsection 3.4 : $K = K_\theta$ in each cell by setting $K_\theta(y) = \widehat{K} \circ \Phi_\theta(y)$ (remember that $\theta = \theta(x, \omega)$) i.e.

$$(K_\theta)_{ii}(y) = \widehat{K}_{ii} \circ \Phi_\theta(y) = \frac{1}{\sigma\sqrt{2\pi}} \left(e^{-\frac{1}{2}(\frac{\phi_\theta(y_1) - 0.5}{\sigma})^2} + \cdots + e^{-\frac{1}{2}(\frac{\phi_\theta(y_d) - 0.5}{\sigma})^2} \right) + \varsigma$$

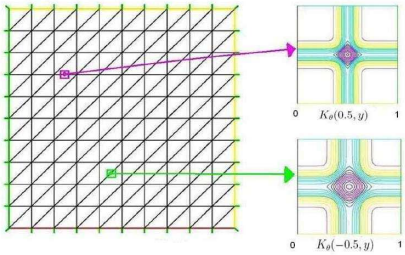

FIG. 4.1. *The domain $\mathcal{D}$ with variable x on the left with example of cell structures on the right with variable y.*

and then, we will solve the corresponding cell problem in order to compute u_ϵ solution of (2.1), by applying the reduced basis method: For all $i \in \{1, \dots, d\}$

$$\begin{cases} -\text{div}(K_\theta(y)(\vec{e}_i + \nabla_y w_i(\theta, y))) = 0 \quad \forall y \in Y =]0,1[^d, \\ w_i(\theta, .) \in H^1_\sharp(Y)/\mathbb{R}. \end{cases} \tag{4.2}$$

In this case, as shown in the figure 4.1, at each quadrature points of $\mathcal{D}$, we choose a random value θ in a compact set $\mathcal{K}$ of $]-2,1[$. Then at each cell, the matrix K is different and leads to different size of pore.
From the last expression of K, we can deduce that the coercivity coefficient of the bilinear form a is very small, since it is of the order of $\alpha_A \simeq \varsigma$. From theorem 3.1 we derive a non pertinent result because the effectivities η_i is bounded by β^{-1}/α_A. To circumvent this problem, we will take into account the fact that

- the permeability constant almost vanishes in some part of the domain of computation
- the cell design is inherited from a change of variable

this allows to map every solution on the reference domain $\hat{\Lambda}$ and introduce, over $\hat{\Lambda}$ a new scalar product

$$[[\hat{w}, \hat{v}]]_{\hat{\mathcal{X}}} = \int_{\hat{\Lambda}} (\hat{K}\hat{\nabla}\hat{w}\hat{\nabla}\hat{v})$$

for all $\hat{w}, \hat{v} \in \hat{\mathcal{X}}$ and we denote by $|||.|||_{\hat{\mathcal{X}}}$ the associated norm.

LEMMA 4.1. *Let us associate to every w and $v \in \mathcal{X}$, the functions $\hat{w} = w \circ \Phi_\theta^{-1}$ and $\hat{v} = v \circ \Phi_\theta^{-1}$, and let us assume that we choose a random value θ in a compact set $\mathcal{K}$ of $]-2,1[$, then the bilinear form $a(w, v; \theta) = \int_Y K_\theta(y)\nabla w(y).\nabla v(y)dy$ is uniformly continuous and elliptic with respect to the previously defined scalar product in the sense that: there exists two constants $C(\mathcal{K})$ and $C'(\mathcal{K})$ such that*

$$\begin{aligned} a(w, v; \theta) &\leq C(\mathcal{K})|||\hat{w}|||_{\hat{\mathcal{X}}}|||\hat{v}|||_{\hat{\mathcal{X}}}, \\ a(w, w; \theta) &\geq C'(\mathcal{K})|||\hat{w}|||_{\hat{\mathcal{X}}}|||\hat{v}|||_{\hat{\mathcal{X}}}. \end{aligned} \tag{4.3}$$

Proof. We use the change of variable based on Φ_θ and write

$$\begin{aligned} a(w,v;\theta) &= \int_Y K_\theta \nabla w.\nabla v = \int_Y (\hat{K}\circ\Phi_\theta).\nabla w.\nabla v \\ &= \int_{\hat{\Lambda}} (\hat{K}\circ\Phi_\theta\circ\ \Phi_\theta^{-1}).\ ((\nabla w)\circ\ \Phi_\theta^{-1}).((\nabla v)\circ\ \Phi_\theta^{-1}).|\mathcal{J}_\theta| \\ &= \int_{\hat{\Lambda}} \hat{K}.((\nabla w)\circ\Phi_\theta^{-1}).((\nabla v)\circ\ \Phi_\theta^{-1})(\phi_\theta^{-1})'(\hat{y}_1)\ \dots\ (\phi_\theta^{-1})'(\hat{y}_d) \\ &= \int_{\hat{\Lambda}} \hat{K}\ \mathcal{J}_\theta.\nabla_{\Phi^{-1}}(w\circ\Phi_\theta^{-1}).\mathcal{J}_\theta.\nabla_{\Phi^{-1}}(v\circ\Phi_\theta^{-1}).(\phi_\theta^{-1})'(\hat{y}_1).\ \dots\ .(\phi_\theta^{-1})'(\hat{y}_d), \end{aligned}$$

with $\mathcal{J}_\theta$ the Jacobian matrix of Φ_θ^{-1}, $|\mathcal{J}_\theta| = (\phi_{\theta y}^{-1})'(\hat{y}_1).\ \dots\ .(\phi_{\theta y}^{-1})'(\hat{y}_d)$, $\nabla_{\Phi^{-1}}$ the gradient with respect to Φ_θ^{-1}. We then proceed

$$\begin{aligned} a(w,v;\theta) &= \int_{\hat{\Lambda}} \hat{K}\mathcal{J}_\theta.\hat{\nabla}\hat{w}.\mathcal{J}_\theta.\hat{\nabla}\hat{v}.(\phi_\theta^{-1})'(\hat{y}_1)\dots(\phi_\theta^{-1})'(\hat{y}_d) \\ &= \Big(\int_{\hat{\Lambda}} \hat{K}_{11}\ \frac{d\hat{w}}{d\hat{y}_1}.\frac{d\hat{v}}{d\hat{y}_1}.((\phi_\theta^{-1})'(\hat{y}_1))^{-1}.(\phi_\theta^{-1})'(\hat{y}_2).\ \dots\ .(\phi_\theta^{-1})'(\hat{y}_d)\Big) + \dots \\ &\qquad + \Big(\int_{\hat{\Lambda}} \hat{K}_{dd}\ \frac{d\hat{w}}{d\hat{y}_d}\frac{d\hat{v}}{d\hat{y}_d}.(\phi_\theta^{-1})'(\hat{y}_1).\ \dots\ .(\phi_\theta^{-1})'(\hat{y}_{d-1}).((\phi_\theta^{-1})'(\hat{y}_d))^{-1}\Big). \end{aligned}$$

And the proof is complete by introducing the constants $C(\mathcal{K})$ (resp. $C'(\mathcal{K})$) as being the maximum (resp. the minimum) value of the quatities

$$(\phi_\theta^{-1})'(\hat{y}_1).(\phi_\theta^{-1})'(\hat{y}_2).\ \dots\ .((\phi_\theta^{-1})'(\hat{y}_i))^{-1}.\ \dots\ .(\phi_\theta^{-1})'(\hat{y}_d)$$

over all possible $1 \le i \le d$ and $\theta \in \mathcal{K}$: i.e. $C'(\mathcal{K}) = \beta_A^{d-1}\zeta_A^{-1}$ and $C(\mathcal{K}) = \beta_A^{-1}\zeta_A^{d-1}$ with $\zeta_A = \max_{y_1\in[0,1]} (\phi_{\theta y}^{-1})'(y_1)$ and $\beta_A = \min_{y_1\in[0,1]} (\phi_{\theta y}^{-1})'(y_1)$. □

In what follows, we shall denote by $\hat{a}(\hat{w},\hat{v},\theta)$ the last bilinear form defined in the reference cell $\hat{\Lambda}$:

$$\begin{aligned} \hat{a}(\hat{w},\hat{v},\theta) &= \Big(\int_{\hat{\Lambda}} \hat{K}_{11}\ \frac{d\hat{w}}{d\hat{y}_1}.\frac{d\hat{v}}{d\hat{y}_1}.((\phi_\theta^{-1})'(\hat{y}_1))^{-1}.(\phi_\theta^{-1})'(\hat{y}_2).\ \dots\ .(\phi_\theta^{-1})'(\hat{y}_d)\Big) + \dots \\ &\qquad + \Big(\int_{\hat{\Lambda}} \hat{K}_{dd}\ \frac{d\hat{w}}{d\hat{y}_d}\frac{d\hat{v}}{d\hat{y}_d}.(\phi_\theta^{-1})'(\hat{y}_1).\ \dots\ .(\phi_\theta^{-1})'(\hat{y}_{d-1}).((\phi_\theta^{-1})'(\hat{y}_d))^{-1}\Big). \end{aligned}$$

4.2. A posteriori error estimator in the degenerate case. In this subsection, we will establish the *a posteriori* errors corresponding to the new inner product.

THEOREM 4.2. *With this new inner product, we define the a posteriori estimate*

$$\hat{\Delta}_{i,N}(\theta) = (\parallel f_i - a(w_{iN}(\theta,.),.;\theta)\parallel_{\hat{\mathcal{X}}'})/C'(\mathcal{K})$$

and the effectivities

$$\hat{\eta}_{i,N}(\theta) = \hat{\Delta}_{i,N}(\theta,.)/\parallel \hat{w}_i(\theta,.) - \hat{w}_{i\mathrm{N}}(\theta,.))||_{\hat{\mathcal{X}}}.$$

We have the inequality

$$1 \leq \hat{\eta}_{i,N}(\theta) \leq \frac{C(\mathcal{K})}{C'(\mathcal{K})}. \tag{4.4}$$

Proof. First, we have:

$$f_i(v;\theta) - a(w_{iN}(\theta,y),v;\theta) = a(w_i(\theta,.) - w_{iN}(\theta,.),v;\theta) \quad \forall v \in \mathcal{X}. \tag{4.5}$$

Then lemma 4.1 and the coercivity of the form a allows us to obtain this inequality:

$$C'(\mathcal{K})|||\hat{w}|||^2_{\hat{\mathcal{X}}} \leq a(w,w;\theta) = \hat{a}(\hat{w},\hat{w};\theta).$$

By replacing w by $w_i(\theta,.) - w_{iN}(\theta,.)$ we obtain:

$$\begin{aligned} C'(\mathcal{K})|||\hat{w}_i(\theta,.) - \hat{w}_{iN}(\theta,.)|||_{\hat{\mathcal{X}}} &\leq \frac{|a(w_i(\theta,.) - w_{iN}(\theta,.), w_i(\theta,.) - w_{iN}(\theta,.);\theta)|}{|||w_i(\theta,.) - w_{iN}(\theta,.)|||_{\hat{\mathcal{X}}}} \\ &\leq \sup_{\hat{v}\in\hat{\mathcal{X}}} \frac{|f_i(v;\theta) - a(w_{iN}(\theta,y),v;\theta)|}{|||\hat{v}|||_{\hat{\mathcal{X}}}} \\ &\leq |||f_i(.;\theta) - a(w_{iN}(\theta,y),.;\theta)|||_{\hat{\mathcal{X}}'}. \end{aligned}$$

The continuity of the linear form a allows us to obtain:
For all $w \in \mathcal{X}, v \in \mathcal{X}$,

$$a(w,v;\theta) \quad \leq C(\mathcal{K})|||\hat{w}|||_{\hat{\mathcal{X}}}|||\hat{v}|||_{\hat{\mathcal{X}}},$$

hence

$$\begin{aligned} |f_i(.;\theta) - a(w_{iN}(\theta,y),.;\theta)| &= |a(w_i(\theta,.) - w_{iN}(\theta,.),v;\theta)| \\ &\leq C(\mathcal{K})|||\hat{w}_i(\theta,.) - \hat{w}_{iN}(\theta,.)|||_{\hat{\mathcal{X}}}|||\hat{v}|||_{\hat{\mathcal{X}}} \end{aligned}$$

which leads to:

$$|||f_i(.;\theta) - a(w_{iN}(\theta,y),.;\theta)|||_{\hat{\mathcal{X}}'} \leq C(\mathcal{K})|||\hat{w}_i(\theta,.) - \hat{w}_{iN}(\theta,.)|||_{\hat{\mathcal{X}}} \tag{4.6}$$

and ends the proof of (4.4). □

This theorem states that the effectivities $\hat{\eta}_{i,N}(\theta)$ are bounded by a term independent of ς. The next theorem gives a bound on $s_{ij,N}$.

THEOREM 4.3. *With this new inner product, the theorem 3.2 becomes*

$$\mid s_{ij}(\theta) - s_{ij,N}(\theta) \mid \leq \hat{\Delta}_{ij,N}(\theta)$$

with:

$$\hat{\Delta}_{ij,N}(\theta) = \frac{||a(w_i(\theta,.) - w_{iN}(\theta,.),.;\theta)||_{\hat{\mathcal{X}}'}||a(w_j(\theta,.) - w_{jN}(\theta,.),.;\theta)||_{\hat{\mathcal{X}}'}}{C'(\mathcal{K})}.$$

Proof. According to the definition of the matrix s and the linearity of the function f we have:

$$\begin{aligned} |s_{ij}(\theta) - s_{ij,N}(\theta)| &= |f_j(w_i(\theta,.) - w_{iN}(\theta,.),.)| \\ &= |a(w_j(\theta,.), w_i(\theta,.) - w_{iN}(\theta,.);\theta)|. \end{aligned} \tag{4.7}$$

The bilinear form a is symmetric as the matrix $A(\theta, y)$. We have:

$$|a(w_j(\theta,.), w_i(\theta,.) - w_{iN}(\theta,.);\theta)| = |a(w_i(\theta,.) - w_{iN}(\theta,.), w_j(\theta,.);\theta)|. \tag{4.8}$$

On the other hand, $w_{jN}(\theta,.) \in \mathcal{X}_{\mathcal{N}}$ and thus

$$|a(w_i(\theta,.) - w_{iN}(\theta,.), w_{jN}(\theta,.);\theta)| = 0,$$

then

$$|a(w_i(\theta,.) - w_{iN}(\theta,.), w_j(\theta,.);\theta)| = |a(w_i(\theta,.) - w_{iN}(\theta,.), w_j(\theta,.) - w_{jN}(\theta,.);\theta)|. \tag{4.9}$$

Using (4.7), (4.8) and (4.9), we obtain:

$$|s_{ij}(\theta) - s_{ij,N}(\theta)| = |a(w_i(\theta,.) - w_{iN}(\theta,.), w_j(\theta,.) - w_{jN}(\theta,.);\theta)|. \tag{4.10}$$

Then

$$\begin{aligned} &|a(w_i(\theta,.) - w_{iN}(\theta,.), w_j(\theta,.) - w_{jN}(\theta,.);\theta)| \\ &\quad \leq |||a(w_i(\theta,.) - w_{iN}(\theta,.),.;\theta)|||_{\hat{\mathcal{X}}'} |||\hat{w}_j(\theta,.) - \hat{w}_{jN}(\theta,.)|||_{\hat{\mathcal{X}}} \end{aligned} \tag{4.11}$$

and

$$\begin{aligned} |||a(w_j(\theta,.) - w_{jN}(\theta,.),.;\theta)|||_{\hat{\mathcal{X}}'} &\geq \frac{|a(w_j(\theta,.) - w_{jN}(\theta,.), w_j(\theta,.) - w_{jN}(\theta,.);\theta)|}{|||\hat{w}_j(\theta,.) - \hat{w}_{jN}(\theta,.)|||_{\hat{\mathcal{X}}}} \\ &\geq C'(\mathcal{K})|||\hat{w}_j(\theta,.) - \hat{w}_{jN}(\theta,.)|||_{\hat{\mathcal{X}}}. \end{aligned} \tag{4.12}$$

which leads to

$$|||\hat{w}_j(\theta,.) - \hat{w}_{jN}(\theta,.)|||_{\hat{\mathcal{X}}} \leq \frac{1}{C'(\mathcal{K})}|||a(w_j(\theta,.) - w_{jN}(\theta,.),.;\theta)|||_{\hat{\mathcal{X}}'}. \tag{4.13}$$

The inequalities (4.11) and (4.13) give the result. □

5. Numerical Results. In this section, we show numerical results in $\mathcal{D} =]0,1[^d$ for $d = 2, 3$, for $\theta \in \mathcal{K} = [-0.4, 0.4]$ and $f = 0$. These numerical computations are performed with the Freefem++ software [20] with classical P1 Lagrange finite elements.

For the implementation of the RBM, we want to note now that if the permeability $K_\theta(y)$ would have been affine as a function of θ, then $a(w, v, \theta)$ would also be affine in θ, resulting in:

$$a(w_{iN}, v;\theta) = \sum_k t_k(\theta) a_k(w_{iN}, v), \tag{5.1}$$

where t_k depends on θ while a_k only depends on w_{iN} and v. Then an extremely efficient offline-online computational strategy may be developed (see [4]). In the offline stage we could have form $a_k(\xi_j, \xi_i), 1 \leq i, j \leq N$; in the online stage we would need only to assemble and invert $a(\xi_j, \xi_i; \theta) = \sum_k t_k(\theta).a_k(\xi_j, \xi_i)$ resulting in computation that would be independent of $\mathcal{N}$ the number of degrees of freedom of the finite element solver. Since $N \leq \mathcal{N}$ large computational savings can be achieved.

Unfortunately, in our case $K_\theta(y)$ is not affine in θ, so we use the empirical interpolation method [4] that recovers the previous online $\mathcal{N}$-independence even in the presence of non-affine parameter dependence. We do not elaborate on this matter since it is quite classical by now.

First, we show the variation in logarithmic scale of:

$$\widehat{\mathcal{A}}_N = \max_{1\leq i\leq d, \theta\in\mathcal{K}} \frac{\hat{\Delta}_N(w_i(\theta,.))}{||\hat{w}_i(\theta,.)||_{\hat{\mathcal{X}}}}$$

with respect of N, when $\varsigma = 10^{-14}$ and 10^{-10}.
Second, we compare this error values in logarithmic scale, of the *a posteriori* estimate of the solution with the new scalar product $\widehat{\mathcal{A}}_N$ and the *a posteriori* estimate of the solution with the original inner product $\mathcal{A}_N = \max_{1\leq i\leq d, \theta\in\mathcal{K}} \frac{\Delta_N(w_i(\theta,.))}{||w_i(\theta,.)||_{\mathcal{X}}}$.

5.1. Results for $d = 2$. The repartition of the permeability is given by the next figure 5.1. We have:

$$\Gamma_D = \Gamma_1 = \{0\}\times]0.35, 0.65[, \text{ with the corresponding data } g_D = 0,$$

and

$$\Gamma_N = \begin{cases} \Gamma_2 = \{1\}\times]0.35, 0.65[, \text{ with he corresponding data } g_N = -1, \\ \Gamma_3 \text{ is the rest of the boundary, with he corresponding data } g_N = 0, \end{cases}$$

hence the flow is going from the right to the left.

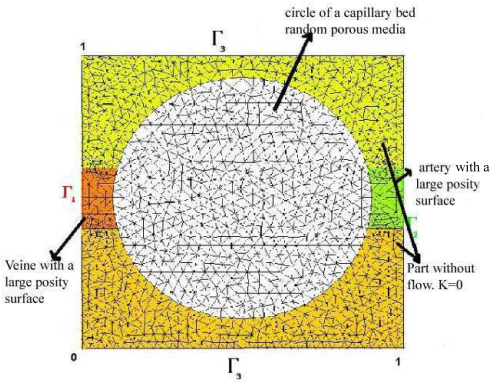

FIG. 5.1. *The domain $\mathcal{D}$ representing the capillary bed, a model of artery on the right and model of vein on the left.*

We conclude from the figures (Fig. 5.2) that, the errors of the solution A_N computed with the original product scalar depend on the values of ς (note that the

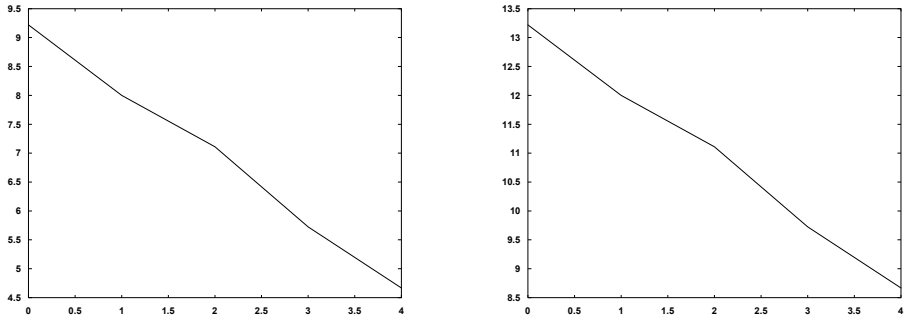

FIG. 5.2. *A_N with respect of N, with $\varsigma = 1e-10$ (left) and $\varsigma = 1e-14$ (right)*

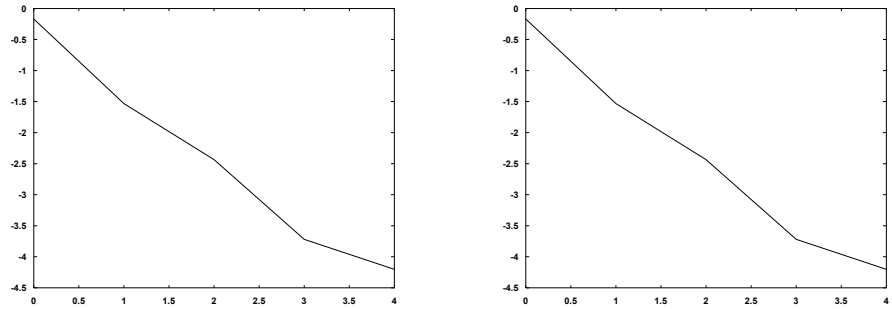

FIG. 5.3. *$\mathcal{A}_N$ with respect of N, with $\varsigma = 1e-10$ (left) and $\varsigma = 1e-14$ (right)*

factor 4 between $\varsigma = 1e-10$ and $\varsigma = 1e-14$ is exactly visible on 5.2). The figure (Fig. 5.3) shows that the errors with the new inner product values, $\widehat{\mathcal{A}}_N$ is not affected by the variation of ς. Moreover, the figures (Fig. 5.2) and (Fig. 5.3) illustrate clearly that the errors of the solutions computed with the new product scalar is much better than the other one. Hence the advantage of this modified approach.

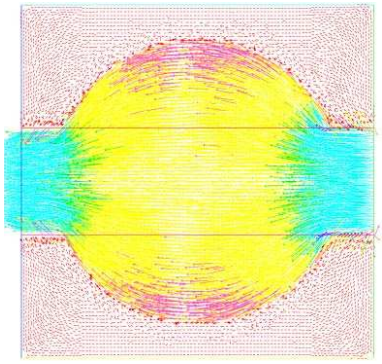

FIG. 5.4. *Modelisation of the velocity*

The color figure 5.4 represents the flow repartition in a porous media for a value of ϵ equal to 0.01

The table (Fig. 5.5) shows the CPU time (in seconds) given by the Freefem++ code

NB	$\mathcal{N}_{\mathcal{Y}}$	$\mathcal{N}$	*RBM*	*FEM*
5	100	121	0.017 s	0.76 s
5	400	121	0.017 s	3. s
5	100	10,201	1.8 s	64. s
5	400	10,201	1.8 s	270. s

FIG. 5.5. *Comparison between the finite element method and the reduced basis method in 2D.*

to approximate the FE matrix for the homogenized problem either with a direct FE approach or with a RB method for a porous medium and for a small ϵ.
As we can see, the RB method is again much faster than the FE method.

In the figures 5.6–5.9 and just for illustrations, we show color results computed on a coarse mesh (not so fine then that used if figure 5.4), for the problem with different boundary conditions to illustrate different models of applications and to show the powerful of this method. The following figures show some applications when the boundary conditions at the input and the output are not aligned.

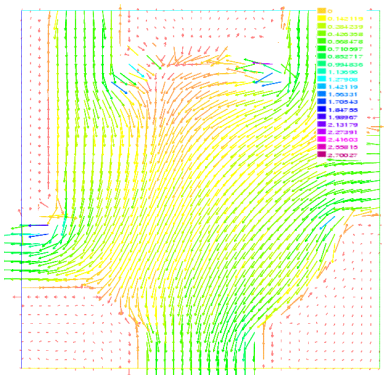

FIG. 5.6.

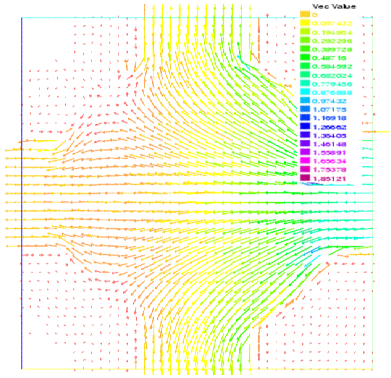

FIG. 5.7.

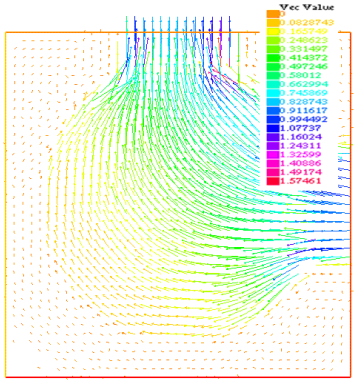

FIG. 5.8.

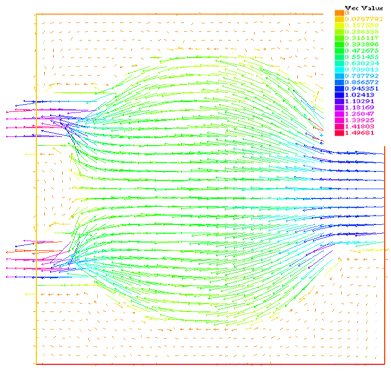

FIG. 5.9.

5.2. Results for $d = 3$. As in the bi-dimensional case, we take the variation of the permeability in the sphere of center $(0.5, 0.5, 0.5)$ and of radius $R = 0.4$ attached to the extremities with cylinders of surface section $S = 0.3$ representing the artery

and the vein. In this case, we take the same boundary conditions as in 2D.

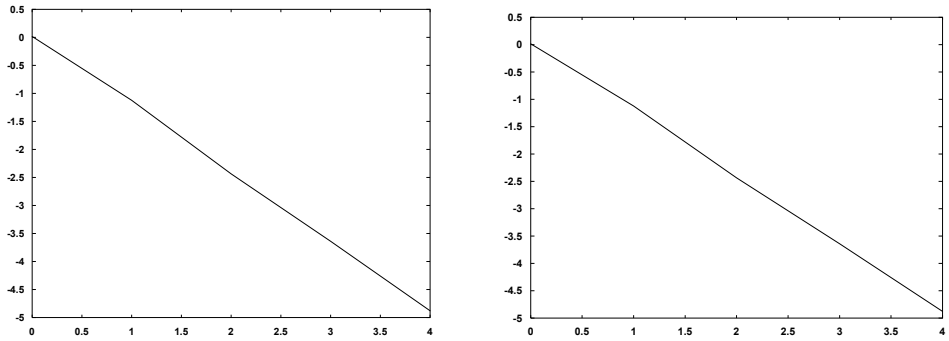

FIG. 5.10. $\mathcal{A}_N$ *with respect of* N*, with* $\varsigma = 1e-10$ *(left) and* $\varsigma = 1e-14$ *(right)*

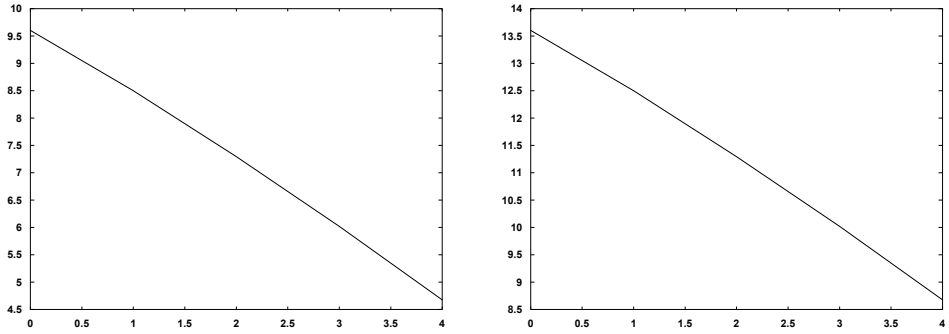

FIG. 5.11. A_N *with respect of* N*, with* $\varsigma = 1e-10$ *(left) and* $\varsigma = 1e-14$ *(right)*

As we see in figures (Fig. 5.10) and (Fig. 5.11), in this case (3D), we have the same conclusions as in the two dimensional case about the new product scalar which gives results independent of ς.

This color figure (Fig. 5.12) represents the flow repartition in a porous media in three dimensional

As in 2D, the table (Fig. 5.13) shows the CPU time (in seconds) given by the Freefem++ code in 3D with the same notations.
As we can see, we have the same remarks concerning the RB method which is faster than the FE method.

Conclusion: In this paper, we use the reduced basis method to solve and speed up the resolution of the Darcy equation in the porous media using the locally homogenization model. This Darcy problem is used as a model for the blood microcirculation in the capillaries. The model is enriched with random properties leading to a random macroscopic stiffness matrix. The microscopic behavior of the micro vessels leads to the introduction of a mathematical model with very small values of the viscosity in some regions. This yields to a non-pertinent *a posteriori* estimates making the construction of the reduced basis problematic. We propose a new microscopic scalar

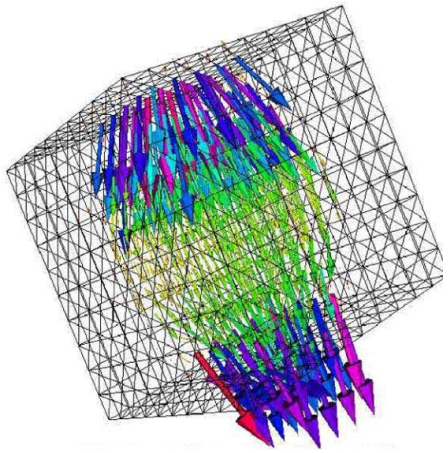

FIG. 5.12. *Modelisation of the velocity in 3D*

NB	$\mathcal{N}_{\mathcal{Y}}$	$\mathcal{N}$	*RBM*	*FEM*
5	125	216	0.13s	41 s
5	1,000	216	0.13 s	326 s
5	125	9,261	8 s	2,500 s
5	1,000	9,261	8 s	20,000 s

FIG. 5.13. *Comparison between the finite element method and the reduced basis method in 3D.*

product to circumvent this difficulty and obtain pertinent results in 2D and 3D. In a future paper we shall analyze more in depth the stochastic behavior (averages, variances ...) of the solutions to this model.

REFERENCES

[1] G. ALLAIRE, *Homogenization and two-scale convergence*, SIAM J. Math. Anal, 23 (1992), pp. 1482–1518.

[2] G. ALLAIRE AND R. BRIZZI, *A multiscale finite element method for numerical homogenization*, SIAM MMS, 4 (2005), pp. 790-812.

[3] N. BAKHVALOV, G. PANASENKO, *Homogenization: averaging processes in periodic media*, Mathematics and its applications, vol.36, Kluwer Academic Publishers, Dordrecht (1990).

[4] M. BARRAULT, Y. MADAY, NGOC CUONG NGUYEN, ANTHONY T. PATERA, *An 'empirical interpolation' method: application to efficient reduced-basis discretization of partial differential equations*, C. R. Acad. Sci. Paris, Ser. I 339 (2004) pp. 667-672.

[5] D. BAUER, R. GREBE AND A. EHRLACHER, *First phase microcirculatory reaction to mechanical skin irritation:a three layer model of a compliant vascular tree*, J Theor Biol., 232(2), (2005), pp. 249–60.

[6] D. BAUER, R. GREBE, A. EHRLACHER,*A three-layer continuous model of porous media to describe the first phase of skin irritation*, J Theor Biol., 232(3), (2005), pp. 347–62.

[7] A. BENSOUSSAN, J. L. LIONS, AND G. PAPANICOLAOU, *Asymptotic analysis for periodic structures, vol. 5 of Studies in Mathematics and its applications,*, North-Holland Publisher Company, 1978.

[8] X. BLANC, C. LE BRIS, AND P. L. LIONS, *Une variante de la theorie de l'homogénéisation stochastique des opérateurs elliptiques*, C.R. Acad. Sci. Paris, 343 (2006), pp. 717–724.

[9] A. BOURGEAT, A. MIKELIC , A. PIATNITSKI, *On the double porosity model of single phase flow in random media*, Asymptotic Analysis , Vol. 34 (2003), p. 311-332.

[10] A.BOURGEAT, A.MIKELIC, S.WRIGHT, *On the Stochastic Two-Scale Convergence in the Mean and Applications*, Journal fur die reine und angewandte Mathematik (Crelles Journal),

Vol. 456 (1994), pp. 19 51.
[11] A. Bourgeat and A. Piatnitski, *Approximations of effective coefficients in stochastic homogenization*, Ann. I.H. Poincaré, 40 (2004), pp. 153-165.
[12] S. Boyaval, *Reduced-Basis approach for homogenization beyond the periodic setting,* rapport interne, INRIA, 2007.
[13] M. Briane, *Homogenization of a non periodic material*, J. Math. Pures Appl., 73 (1994), pp. 47-66.
[14] C. Chakir and Y. Maday, *Une mthode combine d'lments finis deux grilles/bases rduites pour l'approximation des solutions d'une E.D.P. paramtrique*, Comptes Rendus Mathematique, 374 (2009), pp. 435–440.
[15] R. Costaouec, CLB, F. Legoll, *Approximation numérique dune classe de problèmes en homogénéisation stochastique (Numerical approximation of a class of problems in stochastic homogenization)* , C. R. Acad. Sci. Paris, Série I, vol. 348 (1-2), (2010), pp. 99–103.
[16] W. E, B. Engquist, X. Li, W. Ren, and E. Vanden-Eijnden, *The heterogeneous multiscale method: A review*, Commun. Comput. Phys., 2 (2007), pp. 367-450.
[17] J. P. Fink and W. C. Rheinboldt, *On the error behavior of the reduced basis technique for nonlinear finite element approximations*, Z. Angew. Math. Mech., 63(1), (1983), pp. 21–28.
[18] A. Gloria, *An analytical framework for the numerical homogenization of monotone elliptic operators and quasiconvex energies*, Multiscale Modeling and Simulation, 5 (2006), pp. 996-1043.
[19] M. A. Grepl, Y. Maday, N. C. Nguyen and A. T. Patera, *Efficient reduced-basis treatment of nonaffine and nonlinear partial differential equations* , ESAIM: Mathematical Modelling and Numerical Analysis, 41 , (2007), pp. 575–605.
[20] F. Hecht & O. Pironneau, *FreeFem++*, see: http://www.freefem.org.
[21] T. Y. Hou and X. H. Wu, *A multiscale finite element method for elliptic problems in composite materials and porous media*, J. Comput. Phys., 134 (1997), pp. 169-189.
[22] V. Jikov, S. Kozlov, and O. Oleinik, *Homogenization of differential operators and integral functionals*, Springer, Berlin, 1994.
[23] S. M. Kozlov, *Averaging of random operators*, Math. USSR-Sb., 37 (1980), pp. 167–180.
[24] J. L. Lions, D. Lukkassen, L. E. Persson, and P. Wall, *Reiterated homogenization of monotone operators*, C. R. Acad. Sci. Paris, 330 (2000), pp. 675-680.
[25] F. Murat and L. Tartar, H-convergence, *in Topics in the Mathematical Modeling of Composite Materials*, Progr. Nonlinear Differential Equations Appl. 31, A. Cherkaev and R. Kohn, eds., Birkhaüser, Boston, (1997), pp. 21–43.
[26] G. Nguetseng, *Homogenization of perforated domains beyond the periodic setting*, J. Math. Anal. Appl., 289 (2004), pp. 608–628.
[27] N. C. Nguyen, K. Veroy, and A. T. Patera, *Certified real-time solution of parametrized partial differential equations*, Springer, (2005), pp. 1523-1558. in S. Yip.
[28] A. K. Noor and J. M. Peters, *Reduced basis technique for nonlinear analysis of structures*, AIAA Journal, 18(4), (1980), pp. 455–462.
[29] G. Papanicolaou and S. R. S. Varadhan , *Boundary value problems with rapidly oscillating random coefficients*, In Proc. Colloq. on Random Fields: Rigorous Results in Statistical Mechanics and Quantum Field Theory, J. Fritz, J. L. Lebaritz and D. Szasz, eds, Vol. 10 of Colloquia Mathematica Societ. Janos Bolyai, pp. 835-873.
[30] C. Prud'homme, D. V. Rovas, K. Veroy, L. Machiels, Y. Maday, A. T. Patera, G. Turinici, *Reliable real-time solution of parametrized partial differential equations: Reduced-basis output bound methods* , Journal of Fluids Engineering-Transactions of the ASME, 124 (1), (2002), pp. 70–80.
[31] Vankan W., Huyghe J., Janssen J., Huson A., Hacking W., Schreiner W., *Poroelasticity of saturedsolid with an application to bloodperfusion*, Int. J. Eng. Sci. 34, (1996), pp. 1019–1031.